Virus Infection Causes Dysbiosis to Promote Type 1 Diabetes Onset

Zachary J. Morse[1], Rachel L. Simister[1,2], Sean A. Crowe[1,2#], Marc S. Horwitz[1#], Lisa C. Osborne[1#]

[1] Department of Microbiology & Immunology, Life Sciences Institute, University of British Columbia, Vancouver BC Canada

[2] Department of Earth, Ocean, and Atmospheric Sciences, University of British Columbia, Vancouver BC Canada

[#] Co-corresponding authors made equal contributions

Contact information:
Sean A Crowe: sean.crowe@ubc.ca, 604-827-3827

Marc S Horwitz: mhorwitz@mail.ubc.ca, 604-822-6298

Lisa C Osborne: lisa.osborne@ubc.ca, 604 822-6649

Keywords:
diabetes, virus, microbiome, dysbiosis, autoimmunity

Abstract

Autoimmune disorders like type 1 diabetes (T1D) are complex diseases caused by numerous factors including both genetic variance and environmental influences. Two such exogenous factors, intestinal microbial composition and enterovirus infection, have been independently associated with T1D onset in both humans and animal models. Since environmental factors rarely work in isolation, we examined the cross-talk between the microbiome and Coxsackievirus B4 (CVB4), an enterovirus that accelerates T1D onset in non-obese diabetic (NOD) mice. We demonstrate that CVB4-infection induced restructuring of the intestinal microbiome prior to T1D onset that was associated with thinning of the mucosal barrier, bacterial translocation to the pancreatic lymph node, and increased detection of circulating and intestinal commensal-reactive antibodies. Notably, the CVB4-induced change in community composition was strikingly similar to that of uninfected NOD mice that spontaneously developed diabetes, thus implying a mutual "diabetogenic" microbiome. Furthermore, fecal microbiome transfer (FMT) of the diabetogenic microbiota from CVB4-infected mice was sufficient to enhance T1D susceptibility in naïve NOD recipients. These findings support a model whereby CVB infection disrupts the microbiome and intestinal homeostasis in a way that promotes activation of autoreactive immune cells and T1D.

Introduction

Type 1 diabetes (T1D) is an autoimmune disease that results from activation of self-reactive leukocytes that destroy the insulin-secreting beta cells in the pancreas, leading to a subsequent loss of blood glucose regulation. Like many autoimmune disorders, T1D incidence has increased globally in recent years (1,2). Notably, the concordance rate of T1D in monozygotic twins is ~50% (3), suggesting that genetics and heritability only partially account for the likelihood of developing the disease. Environmental factors, including infection history and the intestinal microbiome, cause extensive variation in the immune system (4) and have been prominently implicated in T1D pathogenesis (5–7).

Both clinical and epidemiological studies show that infections of Coxsackievirus B (CVB) and other enteric viruses play a role in precipitating autoimmunity in T1D-susceptible individuals (8–12). CVB is an enterovirus with a single-stranded RNA genome that is typically transferred via the fecal-oral route in humans. Furthermore, enteric infection and persistent gastrointestinal (GI) inflammation precedes T1D onset in humans, signifying a link between intestinal immunity and altered islet-reactivity (9,13,14). Supporting clinical and epidemiological findings that CVB infection is a risk factor for T1D, we have previously found that CVB4 infection is sufficient to break immune tolerance in non-obese diabetic (NOD) mice to trigger the onset of diabetes autoimmunity by promoting bystander immune activation and innate antiviral responses involving type I interferon production (15–18).

Dysbiosis, defined here as a substantial alteration of the intestinal microbial community and/or its functional capacity in relation to the host, has been shown to contribute to the pathogenesis of

several inflammatory disorders, including T1D (19). Changes in microbial community composition, metabolite production, and the intestinal virome have all been linked to altered susceptibility and immune regulation associated with T1D autoimmunity in both humans and rodent models (20–24). Certain T1D-susceptibility alleles for immune-related loci may promote development of autoimmunity via modulation of the gut microbiome, particularly early in life (21,25). Accordingly, disruption in the intestinal microbiome by infection, diet, antibiotic usage, or other factors, plays a considerable role in precipitating diabetes autoimmunity (26,27).

Immune homeostasis in the gastrointestinal (GI) tract and associated lymphoid tissue (GALT) can modify T1D clinical outcomes, contributing to protection and/or pathogenesis of T1D. For instance, IL-10-expressing type 1 regulatory T cells from the GALT can migrate to the pancreas to induce tolerance (28). Microbial products such as the short-chain fatty acid (SCFA) metabolites, acetate and butyrate, can also limit the frequency of autoreactive T cells in T1D (22). Conversely, intestinal inflammation can promote the presentation of pancreatic self-antigen and activation of autoreactive immune cells, particularly within the pancreatic lymph nodes (PLN) that drain GI and pancreatic tissues (29,30). Previously, murine norovirus infection has been shown to protect against T1D autoimmunity in NOD mice through modification of the microbiota and intestinal immune landscape (31). Collectively, these reports suggest the existence of a gut-pancreas axis linking dysbiosis and inflammatory events within the GI environment to pancreatic immune homeostasis that can shape autoreactive potential within the islet microenvironment (32).

The importance of both the intestinal microbiome and viral infection to T1D pathogenesis is well established in both humans and *in vivo* mouse models, but the intersection of these environmental

risk factors has not been defined. Given previous data demonstrating that CVB4 infection accelerates diabetes onset, that viral infections can cause intestinal dysbiosis (31,33–35), and that dysbiosis also influences T1D pathogenesis (27,36–38); we hypothesized that viral infection may modify the intestinal microbiome in a way that enhances diabetogenic potential. Here, we demonstrate that CVB4 infection of NOD mice with CVB4 elicits reproducible changes to the microbiome that precede T1D onset. Infection also led to a thinner mucosal barrier, impaired epithelial barrier integrity and bacterial translocation that were associated with enhanced humoral recognition of commensal antigen. Further, fecal microbiome transfer (FMT) of pre-diabetogenic feces from CVB4-infected donors was sufficient to enhance T1D susceptibility. Collectively, these data demonstrate that enteroviral infection can shift intestinal microbial community composition and structure in a manner that promotes disease susceptibility and as such creates a potential therapeutic target and/or biomarker for earlier detection of T1D susceptibility and subsequent disease prevention.

Methods

Mice and Infection

Age- and sex-matched non-obese diabetic (NOD) mice born and bred within our animal facility were used for all experiments. Mice were housed in OptiMouse cages with corn cob bedding and up to 5 cage-mates. Mice had ad libitum access to chow and reverse osmosis chlorinated (2-3ppm)-purified water. Housing rooms were kept on a 14.5/9.5-hour light/dark cycle with temperature maintained at 22-25°C and 50-70% humidity. Sentinel mice were placed on dirty bedding and nesting material in experimental rooms and subsequently tested on a quarterly basis for presence of parasites (pinworms and fur/follicular mites, *Pneumocystis* spp. (*carinii, murina*)), bacteria (*Mycoplasma pulmonis*), and viruses (RADIL Comprehensive Panel) including Mouse Hepatitis Virus (MHV) Mouse Minute Virus (MMV), Mouse Parvovirus (NS1 – Generic Parvovirus & MPV 1-5), Theiler's Murine Encephalitis Virus (TMEV), Epizootic Diarrhea of Infant Mice (EDIM), Sendai Virus, Pneumonia Virus of Mice (PVM), Reo3 virus (REO3), Lymphocytic Choriomeningitis Virus (LCMV), Ectromelia virus, Murine Adenovirus I/II (MAV1/MAV11), Polyomavirus. All experiments were performed in compliance with protocols approved by the Animal Care Committee of The University of British Columbia.

Virus stocks for coxsackievirus B4 Edwards strain 2 (CVB4) were prepared as previously described (15). Normoglycemic NOD mice at 11-12 weeks old were injected intraperitoneally with either 400 plaque-forming units (pfu) CVB4 or DMEM vehicle. Non-fasting blood glucose was monitored using a OneTouch LifeScan monitor. Mice were considered diabetic with two consecutive readings above 16.2 mg/dL separated by 24 hours.

Histology

For histological analysis, pancreata were placed in 10% neutral buffered formalin for 20-24 hours and moved to 70% ethanol before paraffin embedding. Longitudinal sections were sliced 5μm thick and stained with hematoxylin-eosin. Degree of insulitis (immune infiltration) was graded where peri-insulitis was < 25% of the islet infiltrated, partial insulitis was 25-75%, and invasive insulitis was >75%. Representative images for insulitis are supplied in Supp. Fig. 1.

Portions of the proximal colon were fixed in methanol-Carnoy's reagent (60% methanol, 30% chloroform, 10% glacial acetic acid) for 18-20 hours before moving tissues to 70% ethanol and sent for paraffin embedding. Cross sections were sliced at 6μm thick and stained with Alcian blue. The width of the mucus layers was measured with ImageJ software.

Bacterial Quantification

Fecal pellets were collected at specified intervals following virus infection (0, 2, 3, 7, 14, and 21 days post-infection (dpi)) and frozen immediately on dry ice before being moved to -80°C for storage. Luminal contents of the intestines were also collected by flushing out the fecal matter in the ileum and the proximal colon using sterile water. Contents were spun at 6000*g* for 15 minutes at 4°C and pellet was used for subsequent DNA extraction and sequencing. DNA was extracted and purified using the DNeasy PowerSoil kit (Qiagen), as per manufacturer's instructions. Purified DNA was stored at -20°C.

Bacterial DNA was quantified by quantitative polymerase-chain reaction (qPCR) using the SsoFast™ EvaGreen assay (Bio-Rad) and a CFX96 Real-Time Detection System (Bio-Rad). Total 16S rRNA gene quantities were targeted using bacterial-specific primers, 27F, (5′-AGAGTTTGATCCTGGCTCAG) and DW519R (5′-GNTT TACCGCGGCKGCTG). Standards for total bacteria quantification were derived from 16S rRNA gene clone libraries using a 16S rRNA from the bacteria SUP05 according to Zaikova et al (39). Bacterial DNA standards, ranging from 10^2-10^8 copies and non-template controls were all run in duplicate. *Bifidobacteria* specific 16S rRNA genes were targeted using primers Bifido5, (5'-GATTCTGGCTCAGGATGAACGC) and Bifido3 (5'-CTGATAGGACGCGACCCCAT) (40). Standards for total quantification were made as in (40), but using a Bifidobacteria 16S rRNA gene amplified from mouse fecal material.

Microbial Community Analyses

Bacterial and archaeal small subunit (SSU) rRNA gene (rDNA) fragments from the extracted genomic DNA were amplified using primers 515F and 806R (41). Sample preparation for amplicon sequencing was performed as described previously (41,42). The amplicon library was analyzed on an Agilent Bioanalyzer using a high-sensitivity dsDNA assay to determine approximate library fragment size and to verify library integrity. Pooled library concentration was

determined using the KAPA library quantification kit for Illumina. Library pools were diluted to 4 nM and denatured into single strands using fresh 0.2 N NaOH as recommended by Illumina. The final library was loaded at a concentration of 8 pM, with an additional PhiX spike-in of 5 to 20%. Sequencing was conducted on an Ilumina miseq.

Bioinformatic Analysis

Sequences were processed using the Quantitative Insights Into Microbial Ecology 2 (QIIME 2) software package (43). Denoising, chimera checking, and clustering were performed using the Divisive Amplicon Denoising Algorithm 2 (DADA2) plugin tool and denoise-paired instruction (44). For taxonomic annotation, the SILVA database (release_138) was used as the reference (45), together with the naïve-Bayes-algorithm-based trained classifier for a taxonomic assignment at 99%, using feature classifier classify-sklearn instructions (https://docs.qiime2.org/2022.2/data-resources/). All data were visualized in R, Excel and GraphPad Prism. For α- and β-diversity measures, all samples were subsampled to the lowest coverage depth and standard indices were calculated in Qiime2. ASV table was imported into the program mothur (46) to conduct further microbial community analysis. A multiple-sample analysis of molecular variance (AMOVA) was used to test the significance of differences between microbial communities, and a statistical analysis, based on Linear discriminant analysis Effect Size (LefSe) (47), was used to test for more nuanced differences in microbial community compositions. Raw sequencing data are available under NCBI BioProject BioProject ID PRJNA855481

Intestinal Permeability Assay

Mice were fasted overnight and gavaged the next morning with 80 mg of 3000-5000 kDa FITC-dextran (Sigma-Aldrich) per 100 g bodyweight. Food was placed back in cages and blood samples were collected 4 hours later by either heart puncture or saphenous vein bleed. Blood was spun at 8000*g* for 13 minutes at room temperature (RT). Cleared serum was diluted 1:1 with sterile PBS and measured fluorometrically using a VarioSkan (Thermo Fisher Scientific) plate reader with an excitation of 485 nm and an emission wavelength of 530 nm. Samples were compared to serially diluted FITC-dextran in mouse serum to determine concentration.

Fecal antigen ELISA

To produce sterile fecal antigen, fecal pellets were collected from naïve NOD mice, homogenized in sterile PBS, strained through a 70 μm filter, and heat killed at 70°C for 10 minutes. Fecal antigen concentration was determined using Pierce BCA Protein Assay Kit (Thermo Fisher Scientific). Immulon IV ELISA (Nunc) plates were coated with 10 μg/mL of fecal antigen in Coat Buffer (0.05M Na_2CO_3, 0.05M $NaHCO_3$, pH 9.6) overnight at 4°C. Plates were washed with 0.05% Tween-20 in PBS and blocked with 5% fetal bovine serum (FBS) in PBS for 1 hour at 37°C. Serum samples collected from naïve NOD mice and CVB4-infected mice were diluted to either 1:50 and 1:100, added to the plates, and incubated for 2 hours at 37°C. Plates were washed and stained with HRP α-mouse IgM, IgG, IgG1, IgG2a, or IgA (Thermo Fisher Scientific) for 1 hour at 37°C. Plates were washed and TMB substrate was added. Reaction was stopped using 2N H_2SO_4 and read immediately at 450 nm on a VarioSkan Plate Reader (Thermo Fisher Scientific).

Gene Expression Analysis

Tissue samples from pancreas, lymph nodes, ileum, and proximal colon were harvested and immediately placed in RNAlater (Qiagen). Samples were kept at 4°C overnight before transferring to -80°C for storage. Samples were thawed and RNA extracted using RNeasy RNA extraction kit (Qiagen) according to manufacturer instructions. Complimentary DNA was made using High-Capacity cDNA Reverse Transcription kit (Qiagen). qPCR reactions were carried out using iQ SYBR Green Supermix (Bio-Rad) and gene expression was measured on a CFX96 Real-Time PCR thermocycler (Bio-Rad). Primers used for qPCR reactions are listed in Supplementary Table 3. All samples were measured in triplicate and target genes were normalized to expression of the house-keeping gene GAPDH. Cycle conditions were followed by melt curve analysis to determine amplicon specificity. Results are represented as relative expression to uninfected control mice.

LPS Assay

Serum from mice was diluted 1:75 in sterile pyrogen-free water and heat-shocked at 70°C for 15 minutes. Sample abundance of bacterial lipopolysaccharide (LPS) was measured using a Pierce Chromogenic Endotoxin Quant Kit (Thermo Fisher Scientific) according to manufacturer's instructions. Standard curve using a known amount of endotoxin was used to determine sample concentration.

225 *Fecal Microbiome Transfers*

226 Fecal microbiome transfer (FMT) was performed as described in Staley *et al* (48). Briefly, 6-week-
227 old NOD mice were placed on a broad-spectrum antibiotic course: "non-absorbable" antibiotics
228 for 7 days, 2 days normal drinking water, "absorbable antibiotics" for 7 days, 2 days normal
229 drinking water, "non-absorbable" antibiotics for 7 days, and finally 2 days on normal drinking
230 water before receiving the FMT. "Non-absorbable" antibiotic cocktail included 1mg/mL of each
231 ertapenum (Invanz), neomycin sulfate, and vancomycin hydrochloride. "Absorbable" antibiotic
232 cocktail included 1 mg/mL of each ampicillin sodium salt, cefoperazone sodium salt, and
233 clindamycin hydrochloride. Donor samples were prepared by homogenizing previously frozen
234 fecal pellets pooled from 4-5 mice in sterile PBS at approximately 1 mg/mL in an anaerobic
235 chamber (5% hydrogen, 95% nitrogen). Homogenized samples were passed through a 70 μm filter
236 to remove debris and centrifuged at 6000*g* for 15 minutes at RT. Supernatant was removed and
237 the pellet resuspended. Bacterial cells were counted using a Beckman-Coulter cell counting
238 chamber and recipient mice gavaged with approximately 10^{10} cells.
239
240 *Isolation of Lymphocytes for Flow Cytometry*

241 Single cell suspensions from spleen, pancreatic lymph nodes (PLN), and ileum were prepared for
242 flow cytometry analysis. Spleen and lymph nodes were mashed through 70 μm cell strainer. Spleen
243 red blood cells were lysed with ammonium-chloride-potassium (ACK) lysis buffer for 10 minutes
244 and washed before being resuspended in sterile FACS buffer (PBS with 2%FBS and 2mM EDTA).
245 Free fat and Peyer's patches were removed from small intestines. The tissue was cut open
246 longitudinally, washed in PBS and placed in cold DMEM with 2% FBS. To remove epithelial
247 cells, intestines were incubated in strip buffer (PBS with 1 mM EDTA, 1 mM dithiothreitol, and
248 5% FBS) and shaken at 180 rpm for 10 minutes at 37°C. Tissues were washed, and again incubated
249 in strip buffer with shaking at 180 rpm for 20 minutes at 37°C. Supernatant was discarded, and
250 tissue digested by incubation in DMEM containing 2% FBS, 0.5 mg/mL collagenase/dispase, and
251 0.02 mg/mL DNase I for 30 minutes at 37°C with shaking at 180 rpm. Supernatant containing
252 lamina propria cells was passed through a 70 μm cell strainer and resuspended in FACS buffer.
253
254
255

Stimulation and Staining of Cells for Flow Cytometry

Cells were stimulated with PMA (10 ng/mL) and ionomycin (500 ng/mL) in the presence of GolgiPlug (1X) and 10% FBS in MEM media for 3-4 hours at 37°C followed by viability using e506 Fixable Viability Dye (eBioscience). Cells were incubated with CD16/CD32 Fc block and extracellular markers were stained with monoclonal antibodies for 20 minutes at 4°C using the following antibodies: CD45 (30-F11), TCRβ (H57-597), CD4 (RM4-5), CD8 (53-6.7), CD19 (1D3). Cells were permeabilized using Foxp3/Transcription Factor Staining kit (eBioscience) and intracellular markers were stained with monoclonal antibodies for 45 minutes at 4°C with FoxP3 (FJK-16S) and IL-10 (JES5-16E3) (All antibodies were from Thermo Fisher Scientific). Cells were resuspended in PBS with 2% NCS and 2 mM EDTA. Samples were collected using Attune NxT Flow Cytometer (Thermo Fisher Scientific) and data analyzed with FlowJo Software (BD Biosciences).

Statistical Analysis

Statistics were performed in GraphPad Prism 9.0 software. For comparison of two normally-distributed data sets a two-tailed, unpaired T test with Welch's correction was used for analysis. For three or more experimental groups, a One-Way ANOVA with Tukey's multiple comparison analysis was used to determine differences. If Brown-Forsythe ANOVA test indicated an unequal variance in standard deviation of experimental groups being compared, a Welsh's ANOVA with Dunnett's T3 multiple comparisons test was used. Bar plots are represented as mean with standard error (SEM), and box and whisker plots indicate median with range unless indicated otherwise in figure legends. Significance is indicated with asterisks, where *$p<0.05$, **$p<0.01$, ***$p<0.001$, and ****$p<0.0001$

Results

Microbial Dysbiosis is a Consequence of Virus Infection

To interrogate the interplay of enteric viral infection and the microbiome in the context of T1D pathogenesis, we infected NOD mice with CVB4 and monitored onset of diabetes by blood glucose measurements taken every 2-3 days. Consistent with previous studies from our group, roughly half (53.8%) of the CVB4-infected mice became diabetic within 2 weeks, while only 5% of their mock-infected (control) counterparts spontaneously developed diabetes over the same period (Fig. 1a). Virus-induced acceleration of T1D onset was also sex-independent and affected both female and male NOD mice equally (Supp. Fig. 1a and 1b). Expectedly, the elevated incidence of diabetes in infected mice also resulted in increased insulitis in the pancreatic islets as determined by histology (Fig 1b).

To directly assess the impact of CVB4 infection on microbial community composition, fecal pellets were longitudinally collected from both naïve (control) and infected mice at 0, 2, 3, 7, 14 and 21 days post-infection (dpi) and used for microbial community profiling based on 16S rRNA gene sequencing (Fig 1c). While the overall bacterial load in fecal material remained the same (Fig. 1d), CVB4-infection caused substantial changes to microbial community composition and structure. Over the course of infection, there was a significant loss of α-diversity in the fecal microbiome (Fig. 1e, Supp. Fig. 2a). Similarly, mice that developed diabetes spontaneously (SD) also experienced a loss of α-diversity compared to normoglycemic control mice (Fig 1e). Principal coordinate analysis (PCoA) showed community composition shifts away from that of baseline uninfected mice (upper right quadrant) over the course of the infection (Fig. 1f). Further stratification of mice by infection status, time-point, and glycemia revealed that there was little

change in microbial community composition in the uninfected control mice that remained non-diabetic and the community structure was stable from day 0 and throughout the 3-week monitoring period (Supp. Table 1). In infected mice, there was no noticeable variation between feces collected in days 0-3 post-CVB4 infection, however by day 7 pi there was a substantial alteration in composition that lasted through the 21-day monitoring period. This shift in gut bacterial communities occurring between 3 and 7 days pi was marked by drastically increased relative abundances of members of the Actinomycetota phylum (Fig. 1g & Supp. Fig. 3). These data indicate that dysbiosis primarily develops between day 3 and day 7 pi, and that the dysbiotic microbial community composition is relatively stable throughout the course of our experiments. Luminal contents taken from the small intestine and proximal colon display a similar dysbiotic profile to that of fecal material and also exhibit a loss of bacterial α-diversity (Supp. Fig. 2b & 2c) suggesting that fecal samples appropriately reflect changes within the GI environment.

Importantly, CVB4-induced dysbiosis was strikingly similar to that of naïve mice which spontaneously developed diabetes (Fig. 1g). In both cases, the appearance of an altered microbiota preceded T1D onset, thereby associating dysbiosis with disease. The CVB4-induced dysbiosis occurred in all NOD mice, even those that remained normoglycemic. Ultimately, T1D is a multifactorial disease where certain hallmarks (e.g., autoantibodies, autoreactive T cells, insulitis, dysbiosis, MHC I and interferon-stimulated gene hyperexpression in the pancreas, etc.) are necessary for, but do not independently dictate, disease incidence. Thus, these data demonstrate that the environmental co-factor CVB4 drives microbiome modifications that are associated with enhanced disease susceptibility.

Prior to disease onset, the fecal microbial community featured an abundance of Bacteriodota and Firmicutes, primarily composed of three genera: *Muribaculaceae*, *Alistipes*, and *Lachnospiraceae* (Supp. Fig. 4). Upon infection, there was an increase in the *Bifidobacteria* (within Actinomycetota phylum) and *Akkermansia* (within the Verrucomicrobiota phylum) genera, which became prominent in both the late timepoints following virus infection (samples taken 7-21 dpi) and diabetes onset (Fig. 1g, Fig 1h, Supp. Fig. 3, & Supp. Fig. 4). Using *Bifidobacterial* abundance as a metric, we identified signs of dysbiosis as early as day 5 pi (Fig. 1h), as measured by qPCR. Compensatory loss of strains within the Firmicutes phylum (Supp. Fig. 3) resulted in an increased Bacteroidota to Firmicutes ratio (Fig. 1i) in infected mice. Overall, these data demonstrate that the accelerated diabetes onset caused by CVB4 infection is preceded by a robust and sustained shift in the intestinal microbiome.

Infected Mice Exhibit Altered Intestinal Physiology and Bacterial Translocation

Given that CVB4 accelerated T1D onset is associated with altered microbial community composition, we assessed whether intestinal physiology was also affected. Notably, deliberate disruption of intestinal integrity is sufficient to activate islet-specific autoreactive T cells within the gut mucosa and accelerate diabetes onset in NOD mice (49). By day 7 pi, a time point that coincides with established microbiome shifts in diabetic mice, serum levels of FITC-dextran were elevated by ~2-fold compared to uninfected, non-diabetic controls, indicating reduced intestinal barrier integrity that was maintained until at least day 14 pi (Fig. 2a). These changes were associated with reduced colonic expression of the gene encoding tight junction-associated protein claudin-1 (*cldn1*) and a slight decrease in tight junction protein-1 (*tjp1*) gene expression (Fig. 2b). A layer of mucus largely comprised of glycoproteins produced by intestinal goblet cells acts as a

347 physical barrier to maintain separation of commensal bacteria and the host epithelium. Notably,
348 CVB4 infection induced a rapid thinning of the colonic mucosal barrier (Fig. 2c) that coincided
349 with altered expression of mucin and antimicrobial peptide (amp) genes within the ileum and
350 proximal colon (Supp. Fig. 5a and b), indicating broad effects on intestinal epithelial cell function
351 within the first week of CVB4 infection of NOD mice that coincide with changes in the intestinal
352 microbiome.
353
354 The CVB4-induced changes in intestinal physiology suggested that colonizing microbes may be
355 more likely to translocate out of the gut and into other tissues. Supporting this hypothesis, we
356 found an increased abundance of bacterial lipopolysaccharide (LPS) detected in the blood as early
357 as day 7 pi that was maintained through day 21 pi, suggesting persistent changes to overall
358 intestinal physiology following CVB4 infection (Fig. 2d). Moreover, elevated levels of bacterial
359 16S rRNA were detected in isolated PLN at day 7 post-CVB4 infection (Fig. 2e). 16S DNA was
360 also slightly elevated, yet not significantly, in the mesenteric (MLN) lymph nodes, suggesting the
361 PLN may be preferentially affected (Fig 3e). Collectively, these data indicate that CVB4 infection
362 contributes to systemic and local inflammation through translocation of bacterial antigen.
363
364 ***CVB4 Modifies Host Responses to Commensal Bacteria***
365 Antibody responses to commensal bacteria are typically triggered following introduction of novel
366 bacteria or by new exposure of microbial antigens to immune cells (50). Notably, dysregulation of
367 anti-commensal antibodies has been associated with T1D autoimmunity in both humans and mice
368 (51,52). To test whether impaired barrier integrity, the restructured microbiome and bacterial
369 translocation in CVB4-infected mice impacted humoral immunity to commensal bacteria, we

assayed the presence of commensal-reactive circulating IgM, IgA, and IgG at days 7, 14, and 21 post-CVB4 infection. Following a transient increase in commensal-specific IgM at day 7 pi, IgG was elevated by day 7 pi until day 21 pi, while IgA levels peaked at day 14 pi and were maintained through day 21 pi (Fig. 3a). Consistent with this, expression of the polymeric Ig receptor (pIgR) increased following infection, signifying accelerated trafficking of immunoglobulins across the epithelial barrier (Fig. 3b). This was reflected in detection of increased commensal-reactive IgA and IgG in the colonic lumen (Fig. 3c) and elevated binding of luminal antibodies to microbes isolated from feces (Fig. 3d), indicating that the increased luminal trafficking of immunoglobulins impacts the binding and neutralization of bacteria within the colon of CVB4-infected mice. Ultimately, the elevated antibody responses to intestinal microbes in response to CVB4 infection may indicate a compensatory reaction by the host to stabilize or limit dysbiosis.

Transfer of an Infection-Induced "Diabetogenic" Microbiome can Promote Autoimmunity

To assess whether the CVB4-induced dysbiotic microbiome contributes to the acceleration of autoimmune diabetes, we first used a course of broad-spectrum antibiotics to deplete the microbial biomass of 6-week-old NOD mice (Fig. 5a) before infecting them with CVB4. We found that a majority (71%) of microbiome-depleted mice succumbed to CVB4 infection within 7-10 days (Supp. Fig. 6), thus confounding efforts to assess whether the microbiome is necessary for virus-induced autoimmune diabetes acceleration. Therefore, we turned to fecal microbiome transfer (FMT). Following antibiotic-mediated microbiome depletion, naïve mice received an FMT from either naïve (control FMT) or previously CVB4-infected (CVB4 FMT) donors and blood glucose was monitored over the next 5 weeks to measure diabetes onset (Fig. 5a). Donor material from previously infected mice had no detectable virus and resulting FMT recipient mice displayed no

evidence of viral infection. Notably, the fecal microbiome of FMT recipients was similar to the donor material in terms of reduced α-diversity in CVB4 FMT compared to control (Fig. 5b) and overall bacterial community composition (Fig. 5c). Remarkably, female recipients of a CVB4 FMT were significantly more susceptible to autoimmune diabetes (38.8% normoglycemic at 5 weeks post-FMT) as compared to sex-matched recipients of a control FMT (81.8% normoglycemic at 5 weeks post-FMT) (Fig. 5d). However, none of the male mice receiving an FMT from a previously infected donor became diabetic in the 5 weeks following FMT (data not shown). Thus, while viral infection triggers diabetes onset in both female and male mice equally, indirectly induced microbiome-related effects more significantly impact female than male recipients in terms of diabetes induction. As expected, these female recipient mice receiving the CVB4 FMT also displayed greater pancreatic insulitis (Fig. 5e). Overall, the dysbiosis which results from and persists following enteric virus infection can skew host homeostasis to promote the development of diabetes autoimmunity even in the absence of viral infection.

FMT Modifies Intestinal Immunity

To determine how the dysbiotic microbiome of the CVB4 FMT impacts immune homeostasis and contributes to diabetes susceptibility, we characterized responses within the intestine of female FMT recipients. Short-chain fatty acids (SCFAs) produced by commensal microbes through fermentation of dietary fiber activate free-fatty acid receptors including GPR43, GPR41, and GPR109a to promote regulatory immune responses. The most abundantly expressed of these receptors, GPR43, had reduced expression in the CVB4 FMT mice compared to that of the control FMT recipients (Fig. 5a) suggesting reduced SCFA signaling. Since signaling through GPR43 and other free fatty acid receptors is known to affect regulatory immune responses (53,54), we thus

quantified and assessed the function of T1D-protective regulatory T cells (Tregs) within the lamina propria of the small intestine. Mice receiving an FMT of the dysbiotic microbiome had a lower abundance of anti-inflammatory $Foxp3^+$ regulatory $CD4^+$ T cells (Tregs) (Fig. 5b) and reduced capacity for IL-10 cytokine production (Fig. 5c) relative to controls.

Further, gene expression of the cytokine IL-22, which is a crucial regulator of epithelial homeostasis and microbial defense, was reduced in the proximal colon of CVB4 FMT mice (Fig. 6c), relative to the control. While innate immune signaling through toll-like receptors in colonic tissue was not significantly altered (Supp. Fig. 7), CVB4 FMT recipient mice had lower systemic anti-commensal IgG (but not IgA) responses (Fig. 5e) than the controls, indicating that dysbiosis may lead to a reduced capacity for the host to neutralize commensal antigens and maintain homeostasis. Collectively, these results suggest microbiome dysbiosis resulting from CVB4 infection is capable of modifying the intestinal landscape in a way that is sufficient to promote diabetes autoimmunity.

Discussion

Herein, we used a multifaceted approach for examining environmental factors to test how they affect intestinal homeostasis and influence susceptibility to diabetes. Independently, both enterovirus infection and dysbiosis have been frequently linked to T1D onset and are thus considered key environmental factors, but they have yet to be studied together and this precludes analyses of combined effects and cross-talk. Dysbiosis caused by infection can alter the microbiome in a prolonged or sustained way and these changes have downstream effects on the immune system, including heightened inflammation and reduced activation thresholds that can contribute to autoreactivity in humans (55). In this study, we show that CVB4 infection is capable of driving microbiome dysbiosis, disrupting intestinal physiology, promoting bacterial translocation, and altering host responses to commensal bacteria to ultimately promote the onset of autoimmune diabetes in NOD mice.

While microbiome studies display a good deal of heterogeneity depending on populations studied and conditions of the subjects, there are some consistent results that are often associated with T1D that are also evident in mice infected with CVB4. This includes a loss of α-diversity within bacterial communities, increased abundance within the Bacteroidota phylum relative to a decrease in Firmicutes, and alteration of the bacterial metabolome. These changes have been noted in studies examining both humans (23,52) and mouse models (22,56). This similarity suggests infection could be an initiator of the dysbiosis that has been detected in humans prior to T1D development.

Increased gut permeability is associated with a number of different autoimmune diseases including T1D, multiple sclerosis, and systemic lupus erythematosus (57). This permeability has been identified prior to diabetes development in clinical settings as well as in mouse models, suggesting it may serve as a promoter and/or initiator of autoreactivity. Individuals with islet autoimmunity often have deficiencies in intestinal integrity along with mild enteropathy (14,58). In fact, inducing a "leaky gut" is sufficient to trigger development of islet-reactive T cells in BDC2.5 transgenic NOD mice and bacterial translocation has been found to precede diabetes onset and act as a contributor to autoreactivity in NOD mice (49,59,60). Specifically, increased gut permeability can stimulate islet-reactive T cells in the GI environment to migrate to the pancreas and participate in destruction of the insulin-secreting beta cells (49). Since CVB4 infection is able to induce GI permeability, it represents a potential secondary mechanism that can contribute to autoreactivity.

Infection with CVB4 led to a loss of intestinal integrity and bacterial translocation to the PLN. The microbiota of CVB4-infected NOD mice featured increased relative abundance of *Akkermansia muciniphilia,* which is a known mucin-degrading bacterium due to its ability to catabolize glycan. Overgrowth by members of the *Akkermansia* genus is commonly associated with degradation of the epithelial mucosal barrier, suggesting their possible contribution to the diminished intestinal mucus barrier we observed following CVB4 infection. Increased gut permeability leads to elevated risk of bacterial exposure to immune cells residing in both the mucosal and peripheral environments to subsequently promote inflammation. Due to intestinal alteration following CVB4 infection, bacteria are able to escape the GI tract and enter circulation and PLN. Bacterial translocation has been shown to promote diabetes through several mechanisms including via bacterial antigen presentation to autoreactive T cells (49), enhancing inflammation (61), molecular

mimicry (62,63), and directly causing damage within the islet microenvironment (64). Thus, we propose that increased bacterial presence systemically and within the local pancreatic environment following infection may increase activation of islet-specific T and B cells that lead to autoimmune destruction of insulin-producing pancreatic beta cells.

Infection with CVB4 increased production of anti-commensal IgG and IgA antibodies, which typically help maintain GI homeostasis by controlling bacterial colonization and spatial distribution, particularly within mucosal environments (65). Differences in anti-commensal responses may play a role in diabetes development since they have been observed in individuals at greater risk of developing T1D due to presence of autoimmune risk alleles (66). Furthermore, these humoral responses can be specific to certain species of bacteria. For example, variance has been observed in the prevalence of antibodies against different strains of *Bifidobacteria* in young children who went on to develop islet autoimmunity and T1D later in life (67). While further work is needed, this indicates a potential role for the expanded population of *Bifidobacteria* in CVB4-infected NOD mice. Collectively, these data suggest that reactivity to certain commensal microbes may represent a risk factor and/or biomarker for T1D development.

The intestinal microbiome can be detrimental to immune homeostasis, since strain-specific bacteria can elicit T cell polarity into either inflammatory or regulatory pathways to contribute to autoimmunity (68,69). Accordingly, dysbiosis caused by CVB4 infection in mice may alter the antigenic profile of the bacterial milieu to enhance inflammation and/or restrain microbiota-induced tolerization (70). To uncouple antiviral immunity from the immune mechanisms elicited by the resulting dysbiosis, we used an FMT approach. These studies revealed a surprising sex-

specific effect. Although CVB4-induced diabetes is sex-independent, only female NOD mice exhibit enhanced susceptibility to the diabetogenic FMT. This pathogenesis is akin to spontaneous disease onset. Ultimately, the diabetogenic microbiome may be communicating with resident immune cells to reduce regulatory responses within the GI environment thereby altering diabetes susceptibility.

Lower GPR43 expression in the CVB4 FMT mice indicates a reduction in SCFA signalling, suggesting the dysbiotic microbiome following infection may result in decreased metabolite production. Production of SCFAs through fermentation of dietary fibers is one of the most important ways commensal microbes communicate with host cells. These SCFAs are able to regulate production of IL-22 within the GI environment as well as binding to host receptors including free-fatty acid receptors (GPR43, GPR41, GPR109a) responsible for cellular gene transcription and cell metabolism (71,72). SCFAs like butyrate and propionate are known to significantly promote the production, differentiation, and function of intestinal regulatory T cells (22,73,74) and thus may contribute to the reduced regulatory responses we observed in the GALT of CVB4 FMT mice.

We have shown that enteric virus can disrupt the microbiome and GI-related pathology in order to promote onset of diabetes. This signifies dysbiosis can exist as a vestige of past infection with potential to affect future health and disease predisposition. Ultimately, it is necessary to determine how infectious pathogens affect human physiology and the intestinal microbiome to alter susceptibility to autoimmunity. As the prevalence of T1D continues to rise in North America and across the globe, greater knowledge of how different environmental factors individually or in

combination affect the host and how the host responds to shifts in the gut microbiome are needed to guide development of new therapeutic interventions and develop novel approaches for identifying biomarkers of disease susceptibility.

Acknowledgments

Authors acknowledge support from the GenomeBC Sector Innovation Program (LCO, SAC, MSH) and the Canada Research Chair program (LCO, SAC). ZJM was supported by a Four-Year Fellowship (4YF) from UBC. Technical support came from ubcFLOW, animal care staff at the Modified Barrier Facility, and the UBC Sequencing and Bioinformatics Consortium. This work took place on the traditional, ancestral, and unceded territory of the xʷməθkʷəy̓əm (Musqueam) First Nation.

Contributions

All authors conceived the study. MSH, SAC and LCO secured funding to support the study. ZJM performed all in vivo animal studies, analyzed data and produced associated figures. RLS performed all bioinformatic analysis and produced figures related to microbial community compositions. ZJM wrote the manuscript with support from LCO, SAC and MSH.

Conflict of Interest

Authors have no conflicts to disclose.

Figures

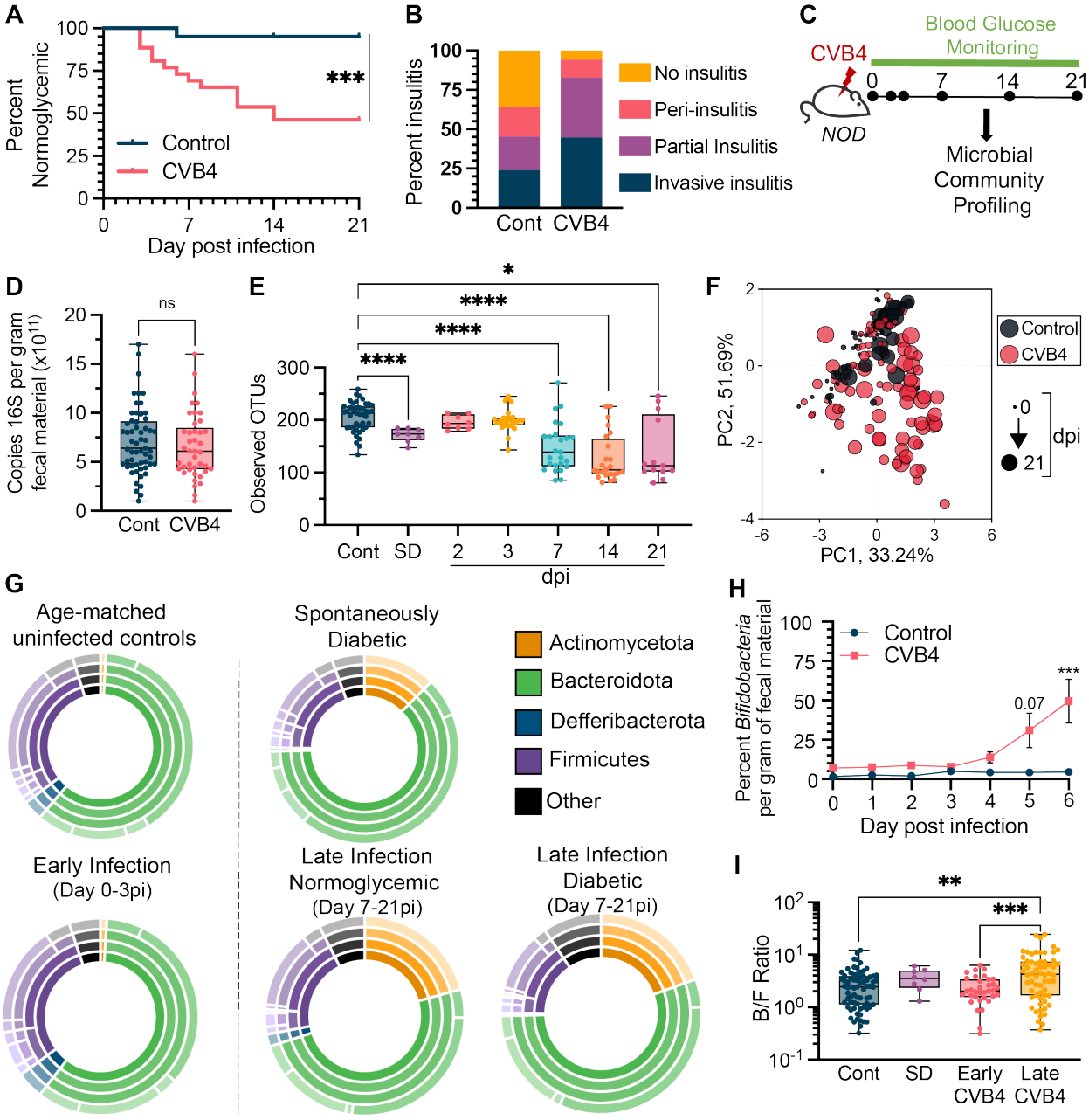

Figure 1. CVB4 infection promotes diabetes incidence and alters gut microbial composition. (A) Diabetes incidence in uninfected control (n = 20) vs. CVB4-infected (n = 26) mice as determined by blood glucose measurement. (B) Degree of pancreatic insulitis as (at day 21 pi) determined by histology. (C) Timeline of microbial community profiling. (D) Copies of 16S genes per gram of fecal material as measured by qPCR. (E) α-diversity (Observed number of OTUs) in bacterial communities following CVB4 infection. Control group includes baseline samples from all mice in the experiment on day 0 prior to mock or CVB4 infection. (F) Principal component analysis (PCoA) of microbial community compositions. (G) The relative abundance of bacterial

taxa within experimental groups. Inner rings indicate composition on a phylum level and each subsequent ring represents a lower taxonomic level (class, order, family). (H) Copies of *Bifidobacterial* genes per gram of fecal material over the first 6 days of infection as measured by qPCR. (I) Ratio of Bacteroidota to Firmicutes abundance in fecal pellets of control, spontaneously diabetic (SD) and CVB4-infected mice at days 0-3 pi (early infection) and 7-21 pi (late infection). Data are representative of at least three independent experiments. * $P \leq 0.05$ was considered statistically significant; ** $P \leq 0.01$, *** $P \leq 0.001$; **** $P \leq 0.0001$, ns = not significant.

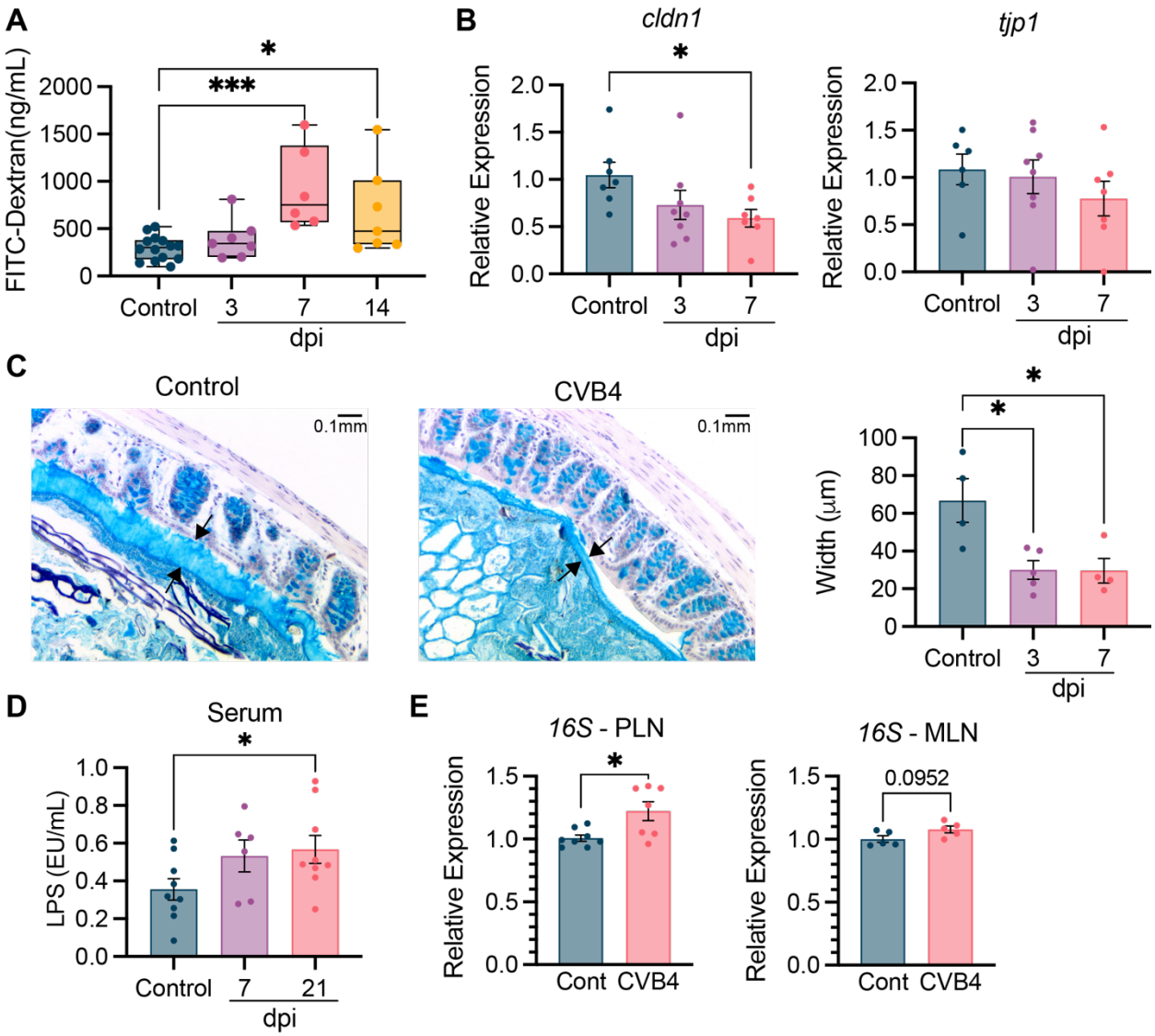

Figure 2. CVB4 infection alters intestinal physiology and causes bacterial translocation. NOD mice (11-12 weeks) were infected with 400 pfu CVB4 intra-peritoneally. (A) Intestinal permeability, based on detection of orally gavaged FITC-Dextran (4 kD) in the serum. (B) Gene expression levels of tight junction-related proteins claudin 1 and tight junction protein 1 in the proximal colon of naïve and CVB4-infected mice. Target gene expression was normalized to GAPDH and expressed relative to uninfected control mice. (C) Representative images of Alcian Blue stained mucus (between arrows) from control and CVB4-infected mice (left) and quantification of mucus width (right). (D) LPS endotoxin levels in the serum. (E) Detection of 16S rRNA in the MLN and PLN of control and CVB4-infected mice (day 7 pi) as determined by qPCR. Intestinal permeability is represented as median with range. All other results are expressed as the mean ± SEM. * $P \leq 0.05$ was considered statistically significant; ** $P \leq 0.01$, *** $P \leq 0.001$.

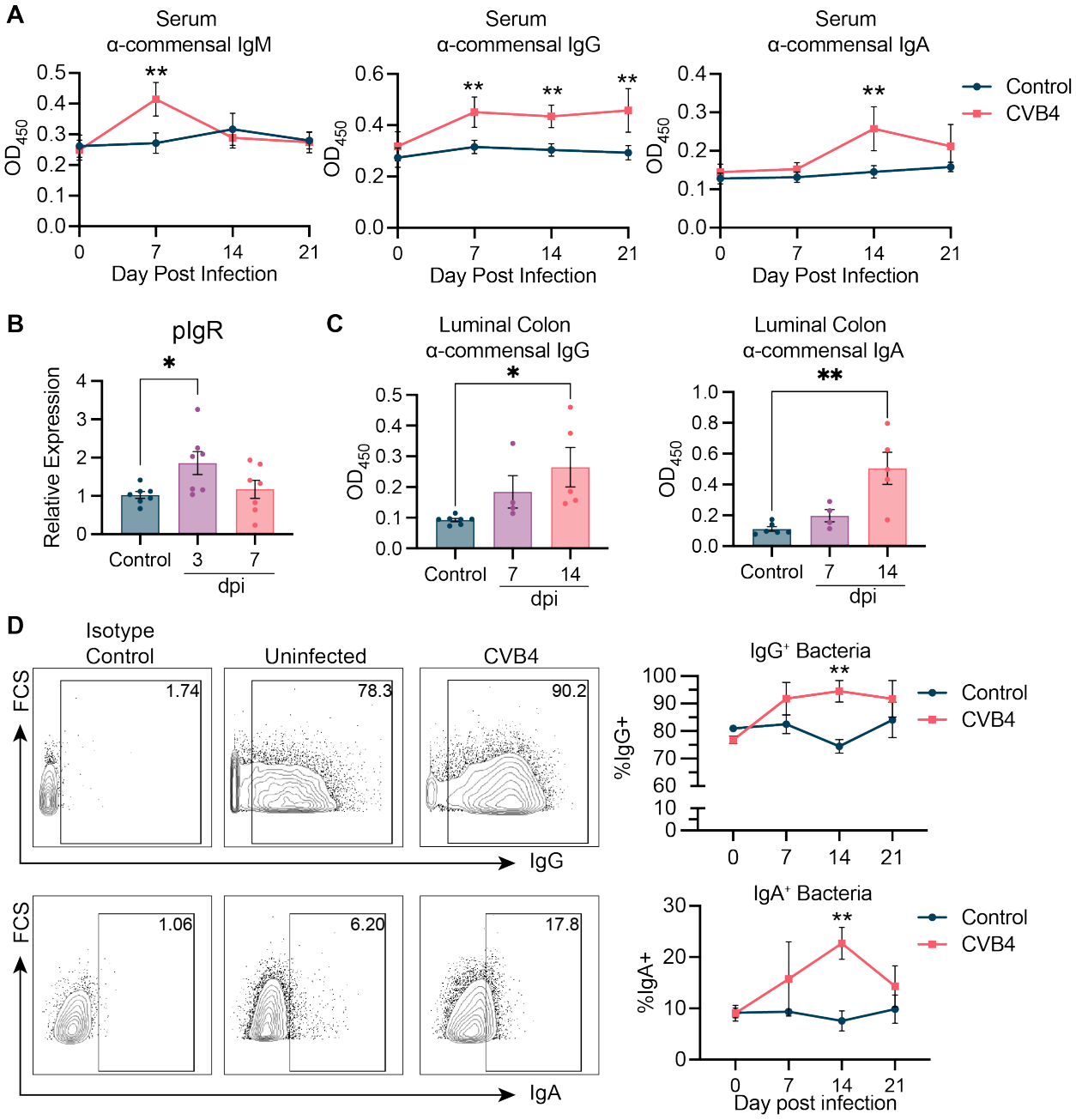

Figure 3. Host responses to commensal microbes is altered following infection. (A) Abundance of bacterial antigen-specific IgM, IgG, or IgA in the serum as measured by ELISA (n = 5 mice per group). (B) Relative expression of polymeric Ig receptor in the small intestine as determined by RT-qPCR. (C) Colonic luminal IgA and IgG reactivity to bacterial antigen as measured by ELISA. (D) Flow cytometry of bacteria from the feces of infected mice indicating proportion of microbes coated with either IgG (top) or IgA (bottom) antibodies. Representative flow plots showing gating of IgG and IgA bound microbes (left), and quantification on the right (n = 4 mice per group). Results are expressed as the mean ± SEM. * $P \leq 0.05$ was considered statistically significant; ** $P \leq 0.01$.

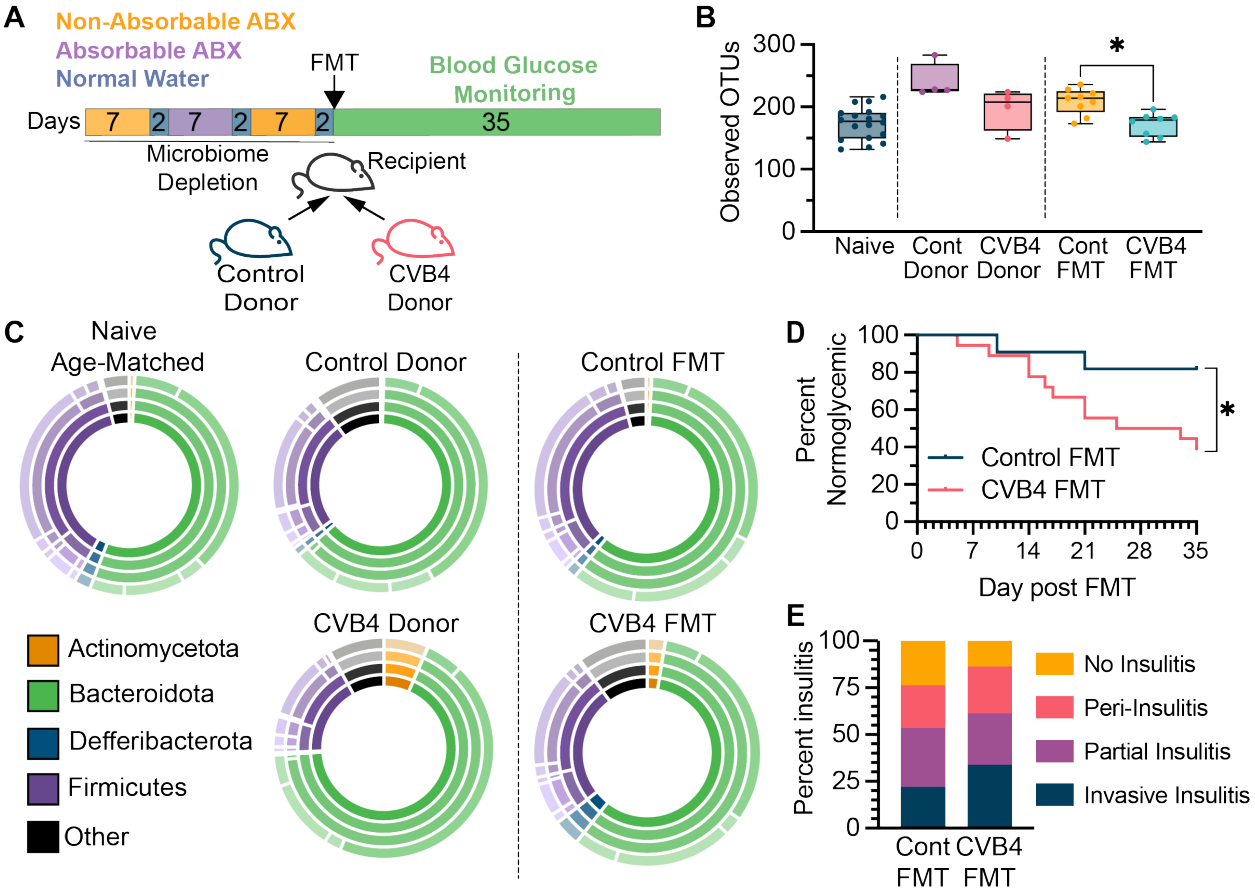

Figure 4. FMT of diabetogenic microbiome in antibiotic depleted mice is able to promote diabetes autoimmunity (A) Experimental design for antibiotic depletion of recipients followed by FMT from donor mice. (B) Microbial diversity in reconstituted FMT recipients. (C) The relative abundance of bacterial taxa within FMT recipient mice. Inner layer = phyla, concentric rings moving out represent lower taxonomic class (class, order, family) (D) Diabetes incidence in mice receiving FMT from either control (n = 11) or a previously infected donor (n = 18) collected at day 14 pi. (E) Insulitis levels in mice receiving FMTs at 5 weeks post FMT. All data in this figure is representative of four independent experiments. A total of four donor pairs (control vs CVB4-infected) were tested. * $P \leq 0.05$ was considered statistically significant.

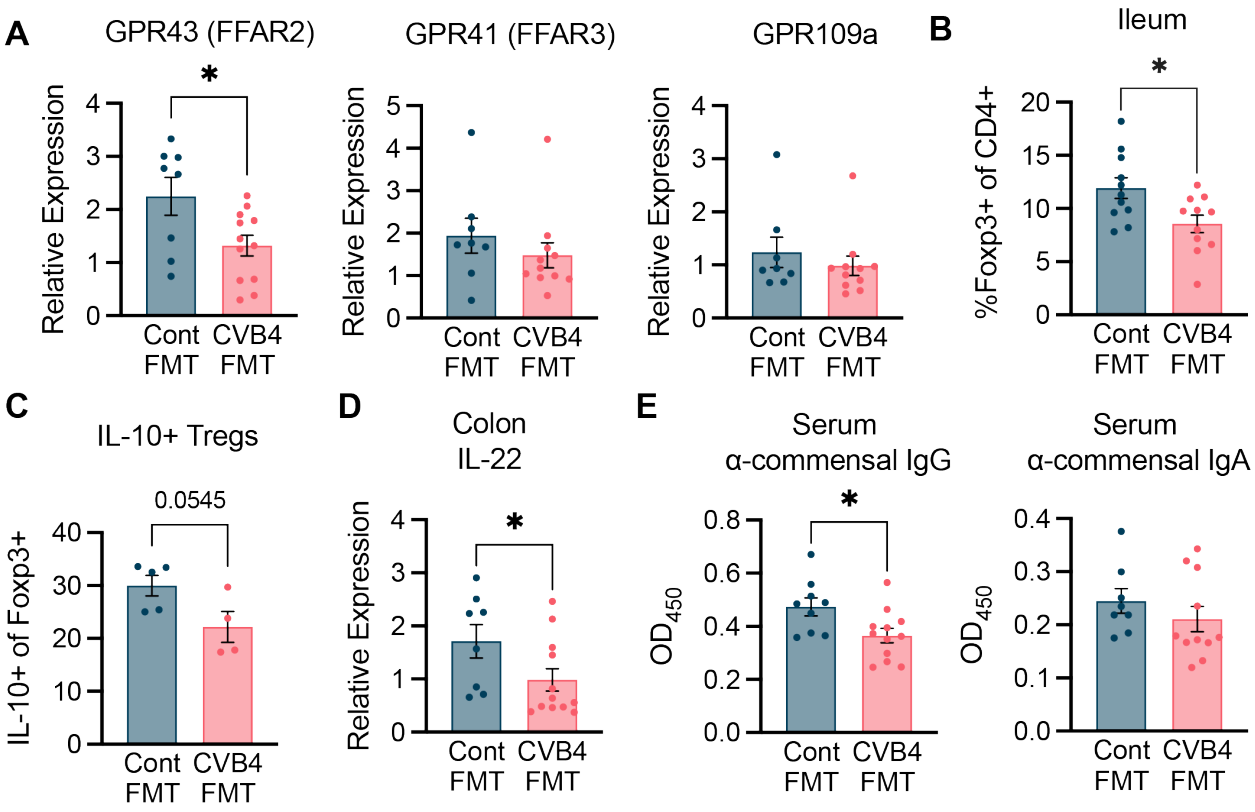

Figure 5. FMT recipient mice have altered intestinal immunity (A) Expression of free fatty acid receptors in the proximal colon of FMT recipient mice. (B) Abundance of $CD4^{+}Foxp3^{+}$ regulatory T cells in the ileum of FMT mice. (C) Expression of IL-10 in the intestinal Tregs. (D) Expression of IL-22 in the proximal colon measured by RT-qPCR. Results were normalized to GAPDH and expressed as relative expression compared to age-matched naïve controls. (E) Abundance of anti-commensal antibodies in the serum of FMT recipient mice as measured by ELISA. * $P \leq 0.05$ was considered statistically significant.

608 **References:**
609
610 1. Ingelfinger JR, Jarcho JA. Increase in the Incidence of Diabetes and Its Implications. N Engl
611 J Med. 2017 Apr 13;376(15):1473–4.

612 2. Long AE, Gillespie KM, Rokni S, Bingley PJ, Williams AJK. Rising Incidence of Type 1
613 Diabetes Is Associated With Altered Immunophenotype at Diagnosis. Diabetes. 2012
614 Mar;61(3):683–6.

615 3. Redondo MJ, Jeffrey J, Fain PR, Eisenbarth GS, Orban T. Concordance for islet
616 autoimmunity among monozygotic twins. N Engl J Med. 2008 Dec 25;359(26):2849–50.

617 4. Brodin P, Jojic V, Gao T, Bhattacharya S, Angel CJL, Furman D, et al. Variation in the
618 Human Immune System Is Largely Driven by Non-Heritable Influences. Cell. 2015 Jan
619 15;160(1):37–47.

620 5. Aw W, Fukuda S. Understanding the role of the gut ecosystem in diabetes mellitus. J Diabetes
621 Investig. 2017 Apr 8;

622 6. Knip M, Simell O. Environmental triggers of type 1 diabetes. Cold Spring Harb Perspect Med.
623 2012 Jul;2(7):a007690.

624 7. van der Werf N, Kroese FGM, Rozing J, Hillebrands JL. Viral infections as potential triggers
625 of type 1 diabetes. Diabetes Metab Res Rev. 2007 Mar;23(3):169–83.

626 8. Nekoua MP, Alidjinou EK, Hober D. Persistent coxsackievirus B infection and pathogenesis
627 of type 1 diabetes mellitus. Nat Rev Endocrinol. 2022 Jun 1;1–14.

628 9. Honkanen H, Oikarinen S, Nurminen N, Laitinen OH, Huhtala H, Lehtonen J, et al. Detection
629 of enteroviruses in stools precedes islet autoimmunity by several months: possible evidence
630 for slowly operating mechanisms in virus-induced autoimmunity. Diabetologia. 2017 Mar
631 1;60(3):424–31.

632 10. Oikarinen M, Tauriainen S, Oikarinen S, Honkanen T, Collin P, Rantala I, et al. Type 1
633 diabetes is associated with enterovirus infection in gut mucosa. Diabetes. 2012
634 Mar;61(3):687–91.

635 11. Oikarinen S, Martiskainen M, Tauriainen S, Huhtala H, Ilonen J, Veijola R, et al. Enterovirus
636 RNA in Blood Is Linked to the Development of Type 1 Diabetes. Diabetes. 2011
637 Jan;60(1):276–9.

638 12. Krogvold L, Edwin B, Buanes T, Frisk G, Skog O, Anagandula M, et al. Detection of a low-
639 grade enteroviral infection in the islets of langerhans of living patients newly diagnosed
640 with type 1 diabetes. Diabetes. 2015 May;64(5):1682–7.

641 13. Stene LC, Oikarinen S, Hyöty H, Barriga KJ, Norris JM, Klingensmith G, et al. Enterovirus
642 infection and progression from islet autoimmunity to type 1 diabetes: the Diabetes and
643 Autoimmunity Study in the Young (DAISY). Diabetes. 2010 Dec;59(12):3174–80.

644 14. Harbison JE, Roth-Schulze AJ, Giles LC, Tran CD, Ngui KM, Penno MA, et al. Gut
645 microbiome dysbiosis and increased intestinal permeability in children with islet
646 autoimmunity and type 1 diabetes: A prospective cohort study. Pediatr Diabetes. 2019
647 Aug;20(5):574–83.

648 15. Horwitz MS, Bradley LM, Harbertson J, Krahl T, Lee J, Sarvetnick N. Diabetes induced by
649 Coxsackie virus: initiation by bystander damage and not molecular mimicry. Nat Med.
650 1998 Jul;4(7):781–5.

651 16. Horwitz MS, Ilic A, Fine C, Rodriguez E, Sarvetnick N. Presented antigen from damaged
652 pancreatic beta cells activates autoreactive T cells in virus-mediated autoimmune diabetes. J
653 Clin Invest. 2002 Jan;109(1):79–87.

654 17. Lincez PJ, Shanina I, Horwitz MS. Reduced expression of the MDA5 Gene IFIH1 prevents
655 autoimmune diabetes. Diabetes. 2015 Jun;64(6):2184–93.

656 18. Morse ZJ, Horwitz MS. Innate Viral Receptor Signaling Determines Type 1 Diabetes Onset.
657 Front Endocrinol. 2017;8:249.

658 19. Brown EM, Kenny DJ, Xavier RJ. Gut Microbiota Regulation of T Cells During
659 Inflammation and Autoimmunity. Annu Rev Immunol. 2019;37(1):599–624.

660 20. Vehik K, Lynch KF, Wong MC, Tian X, Ross MC, Gibbs RA, et al. Prospective virome
661 analyses in young children at increased genetic risk for type 1 diabetes. Nat Med. 2019
662 Dec;25(12):1865–72.

663 21. Mullaney JA, Stephens JE, Costello ME, Fong C, Geeling BE, Gavin PG, et al. Type 1
664 diabetes susceptibility alleles are associated with distinct alterations in the gut microbiota.
665 Microbiome. 2018 Feb 17;6:35.

666 22. Mariño E, Richards JL, McLeod KH, Stanley D, Yap YA, Knight J, et al. Gut microbial
667 metabolites limit the frequency of autoimmune T cells and protect against type 1 diabetes.
668 Nat Immunol. 2017 May;18(5):552–62.

669 23. Zhao G, Vatanen T, Droit L, Park A, Kostic AD, Poon TW, et al. Intestinal virome changes
670 precede autoimmunity in type I diabetes-susceptible children. Proc Natl Acad Sci. 2017 Jul
671 10;201706359.

672 24. Filyk HA, Osborne LC. The Multibiome: The Intestinal Ecosystem's Influence on Immune
673 Homeostasis, Health, and Disease. EBioMedicine. 2016 Nov 1;13:46–54.

674 25. Silverman M, Kua L, Tanca A, Pala M, Palomba A, Tanes C, et al. Protective major
675 histocompatibility complex allele prevents type 1 diabetes by shaping the intestinal
676 microbiota early in ontogeny. Proc Natl Acad Sci. 2017 Sep 5;114(36):9671–6.

677 26. Dedrick S, Sundaresh B, Huang Q, Brady C, Yoo T, Cronin C, et al. The Role of Gut
678 Microbiota and Environmental Factors in Type 1 Diabetes Pathogenesis. Front Endocrinol

679 [Internet]. 2020 [cited 2022 Jun 30];11. Available from:
680 https://www.frontiersin.org/article/10.3389/fendo.2020.00078

681 27. Vatanen T, Franzosa EA, Schwager R, Tripathi S, Arthur TD, Vehik K, et al. The human gut
682 microbiome in early-onset type 1 diabetes from the TEDDY study. Nature.
683 2018;562(7728):589–94.

684 28. Yu H, Gagliani N, Ishigame H, Huber S, Zhu S, Esplugues E, et al. Intestinal type 1
685 regulatory T cells migrate to periphery to suppress diabetogenic T cells and prevent
686 diabetes development. Proc Natl Acad Sci U S A. 2017 Sep 26;114(39):10443–8.

687 29. Turley SJ, Lee JW, Dutton-Swain N, Mathis D, Benoist C. Endocrine self and gut non-self
688 intersect in the pancreatic lymph nodes. Proc Natl Acad Sci U S A. 2005 Dec
689 6;102(49):17729–33.

690 30. Pöysti S, Toivonen R, Takeda A, Silojärvi S, Yatkin E, Miyasaka M, et al. Infection with the
691 enteric pathogen C. rodentium promotes islet-specific autoimmunity by activating a
692 lymphatic route from the gut to pancreatic lymph node. Mucosal Immunol. 2022
693 May;15(3):471–9.

694 31. Pearson JA, Tai N, Ekanayake-Alper DK, Peng J, Hu Y, Hager K, et al. Norovirus Changes
695 Susceptibility to Type 1 Diabetes by Altering Intestinal Microbiota and Immune Cell
696 Functions. Front Immunol. 2019;10(2654).

697 32. Burrows MP, Volchkov P, Kobayashi KS, Chervonsky AV. Microbiota regulates type 1
698 diabetes through Toll-like receptors. Proc Natl Acad Sci U S A. 2015 Aug
699 11;112(32):9973–7.

700 33. Vujkovic-Cvijin I, Dunham RM, Iwai S, Maher MC, Albright RG, Broadhurst MJ, et al.
701 Dysbiosis of the gut microbiota is associated with HIV disease progression and tryptophan
702 catabolism. Sci Transl Med. 2013 Jul 10;5(193):193ra91.

703 34. Inoue T, Nakayama J, Moriya K, Kawaratani H, Momoda R, Ito K, et al. Gut Dysbiosis
704 Associated With Hepatitis C Virus Infection. Clin Infect Dis Off Publ Infect Dis Soc Am.
705 2018 31;67(6):869–77.

706 35. Yildiz S, Mazel-Sanchez B, Kandasamy M, Manicassamy B, Schmolke M. Influenza A virus
707 infection impacts systemic microbiota dynamics and causes quantitative enteric dysbiosis.
708 Microbiome. 2018 10;6(1):9.

709 36. Zhou H, Sun L, Zhang S, Zhao X, Gang X, Wang G. Evaluating the Causal Role of Gut
710 Microbiota in Type 1 Diabetes and Its Possible Pathogenic Mechanisms. Front Endocrinol.
711 2020;11(125).

712 37. Alkanani AK, Hara N, Gottlieb PA, Ir D, Robertson CE, Wagner BD, et al. Alterations in
713 Intestinal Microbiota Correlate With Susceptibility to Type 1 Diabetes. Diabetes. 2015 Oct
714 1;64(10):3510–20.

715 38. Kostic AD, Gevers D, Siljander H, Vatanen T, Hyötyläinen T, Hämäläinen AM, et al. The
716 dynamics of the human infant gut microbiome in development and in progression toward
717 type 1 diabetes. Cell Host Microbe. 2015 Feb 11;17(2):260–73.

718 39. Zaikova E, Walsh DA, Stilwell CP, Mohn WW, Tortell PD, Hallam SJ. Microbial
719 community dynamics in a seasonally anoxic fjord: Saanich Inlet, British Columbia. Environ
720 Microbiol. 2010 Jan;12(1):172–91.

721 40. Gueimonde M, Tölkkö S, Korpimäki T, Salminen S. New real-time quantitative PCR
722 procedure for quantification of bifidobacteria in human fecal samples. Appl Environ
723 Microbiol. 2004 Jul;70(7):4165–9.

724 41. Apprill A, McNally S, Parsons R, Weber L. Minor revision to V4 region SSU rRNA 806R
725 gene primer greatly increases detection of SAR11 bacterioplankton. Aquat Microb Ecol.
726 2015 Jun 4;75(2):129–37.

727 42. Caporaso JG, Lauber CL, Walters WA, Berg-Lyons D, Lozupone CA, Turnbaugh PJ, et al.
728 Global patterns of 16S rRNA diversity at a depth of millions of sequences per sample. Proc
729 Natl Acad Sci. 2011 Mar 15;108(supplement_1):4516–22.

730 43. Bolyen E, Rideout JR, Dillon MR, Bokulich NA, Abnet CC, Al-Ghalith GA, et al.
731 Reproducible, interactive, scalable and extensible microbiome data science using QIIME 2.
732 Nat Biotechnol. 2019 Aug;37(8):852–7.

733 44. Callahan BJ, McMurdie PJ, Rosen MJ, Han AW, Johnson AJA, Holmes SP. DADA2: High-
734 resolution sample inference from Illumina amplicon data. Nat Methods. 2016
735 Jul;13(7):581–3.

736 45. Quast C, Pruesse E, Yilmaz P, Gerken J, Schweer T, Yarza P, et al. The SILVA ribosomal
737 RNA gene database project: improved data processing and web-based tools. Nucleic Acids
738 Res. 2013 Jan;41(Database issue):D590–6.

739 46. Schloss PD, Westcott SL, Ryabin T, Hall JR, Hartmann M, Hollister EB, et al. Introducing
740 mothur: Open-Source, Platform-Independent, Community-Supported Software for
741 Describing and Comparing Microbial Communities. Appl Environ Microbiol. 2009
742 Dec;75(23):7537–41.

743 47. Segata N, Izard J, Waldron L, Gevers D, Miropolsky L, Garrett WS, et al. Metagenomic
744 biomarker discovery and explanation. Genome Biol. 2011 Jun 24;12(6):R60.

745 48. Staley C, Kaiser T, Beura LK, Hamilton MJ, Weingarden AR, Bobr A, et al. Stable
746 engraftment of human microbiota into mice with a single oral gavage following antibiotic
747 conditioning. Microbiome [Internet]. 2017 Aug 1 [cited 2019 Feb 28];5. Available from:
748 https://www.ncbi.nlm.nih.gov/pmc/articles/PMC5537947/

749 49. Sorini C, Cosorich I, Lo Conte M, De Giorgi L, Facciotti F, Lucianò R, et al. Loss of gut
750 barrier integrity triggers activation of islet-reactive T cells and autoimmune diabetes. Proc
751 Natl Acad Sci. 2019 Jul 23;116(30):15140–9.

50. Zeng MY, Cisalpino D, Varadarajan S, Hellman J, Warren HS, Cascalho M, et al. Gut Microbiota-Induced Immunoglobulin G Controls Systemic Infection by Symbiotic Bacteria and Pathogens. Immunity. 2016 Mar 15;44(3):647–58.

51. Paun A, Yau C, Meshkibaf S, Daigneault MC, Marandi L, Mortin-Toth S, et al. Association of HLA-dependent islet autoimmunity with systemic antibody responses to intestinal commensal bacteria in children. Sci Immunol. 2019 Feb 1;4(32).

52. Huang J, Pearson JA, Peng J, Hu Y, Sha S, Xing Y, et al. Gut microbial metabolites alter IgA immunity in type 1 diabetes. JCI Insight. 2020 May 21;5(10).

53. Smith PM, Howitt MR, Panikov N, Michaud M, Gallini CA, Bohlooly-Y M, et al. The microbial metabolites, short chain fatty acids, regulate colonic Treg cell homeostasis. Science. 2013 Aug 2;341(6145):10.1126/science.1241165.

54. Sun M, Wu W, Chen L, Yang W, Huang X, Ma C, et al. Microbiota-derived short-chain fatty acids promote Th1 cell IL-10 production to maintain intestinal homeostasis. Nat Commun. 2018 Sep 3;9(1):3555.

55. Morse ZJ, Horwitz MS. Virus Infection Is an Instigator of Intestinal Dysbiosis Leading to Type 1 Diabetes. Front Immunol. 2021;12:4312.

56. Simon MC, Reinbeck AL, Wessel C, Heindirk J, Jelenik T, Kaul K, et al. Distinct alterations of gut morphology and microbiota characterize accelerated diabetes onset in nonobese diabetic mice. J Biol Chem. 2020 Jan 24;295(4):969–80.

57. Mu Q, Kirby J, Reilly CM, Luo XM. Leaky Gut As a Danger Signal for Autoimmune Diseases. Front Immunol. 2017 May 23;8.

58. Bosi E, Molteni L, Radaelli MG, Folini L, Fermo I, Bazzigaluppi E, et al. Increased intestinal permeability precedes clinical onset of type 1 diabetes. Diabetologia. 2006 Dec;49(12):2824–7.

59. Sofi MH, Johnson BM, Gudi RR, Jolly A, Gaudreau MC, Vasu C. Polysaccharide A-Dependent Opposing Effects of Mucosal and Systemic Exposures to Human Gut Commensal Bacteroides fragilis in Type 1 Diabetes. Diabetes. 2019 Oct;68(10):1975–89.

60. Miranda MCG, Oliveira RP, Torres L, Aguiar SLF, Pinheiro-Rosa N, Lemos L, et al. Frontline Science: Abnormalities in the gut mucosa of non-obese diabetic mice precede the onset of type 1 diabetes. J Leukoc Biol. 2019 Sep;106(3):513–29.

61. Costa FRC, Françozo MCS, Oliveira GG de, Ignacio A, Castoldi A, Zamboni DS, et al. Gut microbiota translocation to the pancreatic lymph nodes triggers NOD2 activation and contributes to T1D onset. J Exp Med. 2016 Jun 27;213(7):1223–39.

62. Abdellatif AM, Jensen Smith H, Harms RZ, Sarvetnick NE. Human Islet Response to Selected Type 1 Diabetes-Associated Bacteria: A Transcriptome-Based Study. Front Immunol. 2019;10:2623.

788 63. Tai N, Peng J, Liu F, Gulden E, Hu Y, Zhang X, et al. Microbial antigen mimics activate
789 diabetogenic CD8 T cells in NOD mice. J Exp Med. 2016 19;213(10):2129–46.

790 64. Myers MA, Hettiarachchi KD, Ludeman JP, Wilson AJ, Wilson CR, Zimmet PZ. Dietary
791 microbial toxins and type 1 diabetes. Ann N Y Acad Sci. 2003 Nov;1005:418–22.

792 65. Weis AM, Round JL. Microbiota-antibody interactions that regulate gut homeostasis. Cell
793 Host Microbe. 2021 Mar 10;29(3):334–46.

794 66. Ferreira RC, Pan-Hammarström Q, Graham RR, Gateva V, Fontán G, Lee AT, et al.
795 Association of IFIH1 and other autoimmunity risk alleles with selective IgA deficiency. Nat
796 Genet. 2010 Sep;42(9):777–80.

797 67. Talja I, Kubo AL, Veijola R, Knip M, Simell O, Ilonen J, et al. Antibodies to Lactobacilli
798 and Bifidobacteria in Young Children with Different Propensity to Develop Islet
799 Autoimmunity [Internet]. Journal of Immunology Research. 2014 [cited 2019 Jun 4].
800 Available from: https://www.hindawi.com/journals/jir/2014/325938/

801 68. Krych Ł, Nielsen DS, Hansen AK, Hansen CHF. Gut microbial markers are associated with
802 diabetes onset, regulatory imbalance, and IFN-γ level in NOD mice. Gut Microbes.
803 2015;6(2):101–9.

804 69. Geva-Zatorsky N, Sefik E, Kua L, Pasman L, Tan TG, Ortiz-Lopez A, et al. Mining the
805 Human Gut Microbiota for Immunomodulatory Organisms. Cell. 2017 Feb 23;168(5):928-
806 943.e11.

807 70. Vatanen T, Kostic AD, d'Hennezel E, Siljander H, Franzosa EA, Yassour M, et al. Variation
808 in Microbiome LPS Immunogenicity Contributes to Autoimmunity in Humans. Cell. 2016
809 May 5;165(4):842–53.

810 71. Yang W, Yu T, Huang X, Bilotta AJ, Xu L, Lu Y, et al. Intestinal microbiota-derived short-
811 chain fatty acids regulation of immune cell IL-22 production and gut immunity. Nat
812 Commun. 2020 Dec;11(1):4457.

813 72. Hee B van der, Wells JM. Microbial Regulation of Host Physiology by Short-chain Fatty
814 Acids. Trends Microbiol. 2021 Aug 1;29(8):700–12.

815 73. Jacob N, Jaiswal S, Maheshwari D, Nallabelli N, Khatri N, Bhatia A, et al. Butyrate induced
816 Tregs are capable of migration from the GALT to the pancreas to restore immunological
817 tolerance during type-1 diabetes. Sci Rep. 2020 Nov 5;10(1):19120.

818 74. Smith PM, Howitt MR, Panikov N, Michaud M, Gallini CA, Bohlooly-Y M, et al. The
819 microbial metabolites, short-chain fatty acids, regulate colonic Treg cell homeostasis.
820 Science. 2013 Aug 2;341(6145):569–73.

821